
## Liquid Crystals
Publication details, including instructions for authors and subscription information:
http://www.informaworld.com/smpp/title~content=t713926090

# Dielectric relaxation spectroscopy and electro-optical studies of a new, partially fluorinated orthoconic antiferroelectric liquid crystal material exhibiting V-shaped switching

S. Ghosh[a]; P. Nayek[a]; S. Kr. Roy[a]; Tapas Pal Majumder[b]; R. Dabrowski[c]
[a] Department of Spectroscopy, Indian Association for the Cultivation of Science, Jadavpur, Kolkata, India [b] Department of Physics, University of Kalyani, Kalyani, West Bengal, India [c] Institute of Chemistry, Military University of Technology, Warsaw, Poland

Online publication date: 23 April 2010

**To cite this Article** Ghosh, S. , Nayek, P. , Roy, S. Kr. , Majumder, Tapas Pal and Dabrowski, R.(2010) 'Dielectric relaxation spectroscopy and electro-optical studies of a new, partially fluorinated orthoconic antiferroelectric liquid crystal material exhibiting V-shaped switching', Liquid Crystals, 37: 4, 369 — 375

**To link to this Article: DOI:** 10.1080/02678291003611367
**URL:** http://dx.doi.org/10.1080/02678291003611367

*Liquid Crystals,*
Vol. 37, No. 4, April 2010, 369–375

Taylor & Francis
Taylor & Francis Group

# Dielectric relaxation spectroscopy and electro-optical studies of a new, partially fluorinated orthoconic antiferroelectric liquid crystal material exhibiting V-shaped switching

S. Ghosh[a], P. Nayek[a], S. Kr. Roy[a]*, T.P. Majumder[b] and R. Dabrowski[c]

[a]*Department of Spectroscopy, Indian Association for the Cultivation of Science, Jadavpur, Kolkata 700032, India;* [b]*Department of Physics, University of Kalyani, Kalyani 741235, West Bengal, India;* [c]*Institute of Chemistry, Military University of Technology, 00-908 Warsaw, Poland*

*( Received 18 November 2009; final version received 11 January 2010)*

In this paper we report the results from detailed electro-optical and dielectric studies in various antiferroelectric and ferroelectric phases of an orthoconic antiferroelectric liquid crystal (OAFLC) material . The material possesses high tilt and high spontaneous polarisation. Such an OAFLC, because of its high tilt, provides an excellent dark state. The material exhibits V-shaped switching in the SmC* phase. Dielectric studies reveal the existence of another phase during heating in the range between 78.6 and 92°C which did not appear in the DSC curve and in polarising microscopy. This phase has been identified as the $SmC_\gamma$* phase and is extremely sensitive with respect to the cell conditions, aligning material, purity, etc. Three dielectric modes have been assigned in the above-mentioned temperature range and their origins are discussed.

**Keywords:** antiferroelectric liquid crystal; dielectric spectroscopy; V-shaped switching; ferrielectric phase; orthoconic liquid crystal



## 1. Introduction

The orthoconic antiferroelectric liquid crystal (OAFLC) is a chiral, tilted smectic phase in which the directors in consecutive layers are at right angles to each other. Such OAFLCs are particularly interesting for their unique optical properties such as fast switching time, wide viewing angle, and the ability to achieve a perfect dark state under cross polarisation. Dielectric relaxation spectroscopy has proven to be a powerful technique for identifying the different subphases in antiferroelectric liquid crystal (AFLC) [1–5]. Subphases such as $SmC_\alpha$*, $SmC_\beta$*, and $SmC_\gamma$* were classified according to the number of layers and their orientation in a unit cell, for example $SmC_\beta$* has four layers and $SmC_\gamma$* has three layers in a unit cell. However, the exact structure of the repeating unit has not been clear until now [6]. These subphases can exhibit polarisation between the antiferroelectric and ferroelectric phases, and have a very complex electro-optical signature. They often seem to disappear on decreasing optical purity, i.e. on adding increasing amounts of enantiomers of opposite handedness [7, 8]. Moreover, the cell thickness has a dominant role to play in such phases. An earlier study by Perkowski *et al.* [9] investigated the dielectric properties of OAFLC in a 5-μm cell, but in thin cells, where the surface effect has the dominating influence, the whole phase behaviour is affected and, on occasions, a certain thermodynamic phase is suppressed completely. Therefore, we have used a 10-μm cell for dielectric studies and observed another phase appearing in the temperature range between 78.6 and 92°C during heating which did not appear in the differential scanning calorimetry (DSC) curve.

Recently, Fukuda *et al.* [10] and later Inui *et al.* [11] discovered threshold-less, hysteresis-free V-shaped switching, a new electro-optical behaviour of some particular smectic mixtures. This hysteresis-free transmission-voltage characteristic is very different from the single hysteresis loop of surface-stabilised ferroelectric liquid crystal (SSFLC) and the double hysteresis loop of surface-stabilised antiferroelectric liquid crystal (SSAFLC). Thus, the V-shaped switching response appears to be an extremely attractive effect capable of producing an electro-optical response with greyscale and high contrast [12–16]. The 'electrostatic model' of V-shaped switching was advanced by Clark *et al.* [17] for materials with high spontaneous polarisation in 2000 and is the currently accepted model. Apart from spontaneous polarisation ($P_s$), the effect of dielectric surface layers is also important for observing the V-shaped switching and has been investigated by Rudquist *et al.* [18–20], Park *et al.* [21, 22] Chandani *et al.* [23], Hammarquist [24), Blinov *et al.* [25] and, recently, by Manjuladevi *et al.* [26]. The aim of the present work was to study the detailed dielectric relaxation in a thick cell together with the electro-optical and optical switching behaviour of the OAFLC material.

*Corresponding author. Email: spskr@iacs.res.in

ISSN 0267-8292 print/ISSN 1366-5855 online

DOI: 10.1080/02678291003611367
http://www.informaworld.com

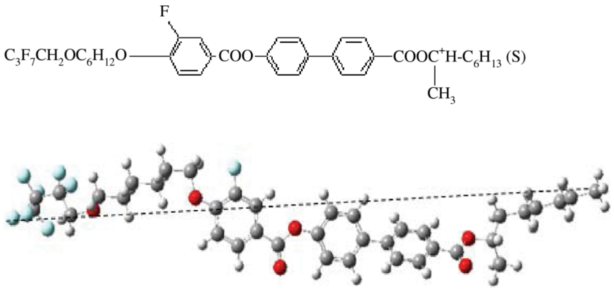


Figure 1. Formula representation and molecular structure of orthoconic antiferroelectric liquid crystal (OAFLC) (colour version online).

## 2. Experimental details

The investigated sample belongs to a new series of partially fluorinated OAFLC synthesised by Morawiak *et al.* [27]. The molecular structure is shown in Figure 1 and its phase sequence is

$$\mathrm{Cr}{<}57.5^\circ\mathrm{C\ SmC_A}^*\ 83.9^\circ\mathrm{C\ SmC}^*\ 110.8^\circ\mathrm{C\ SmA}\ 114.9^\circ\mathrm{C\ Iso}$$

The different liquid crystalline mesophases were identified with the help of polarising microscopy. For the electro-optical measurements, a HP33120A signal generator, F10A voltage amplifier, and DL1620 oscilloscope were used. The spontaneous polarisation was measured using a polarisation reversal method with a triangle-wave voltage of 35 $V_{PP}$ and 10-Hz frequency. The magnitude of the spontaneous polarisation was determined from the current reversal peak. The tilt angle was measured by keeping the cell under a polarising microscope and applying a 40-$V_{PP}$ voltage and a 100-MHz frequency. In order to study the optical switching behaviour, ITO-coated, planar-aligned LC cells (EHC. Ltd. Japan) of 2-μm thickness were used. A photodetector with pre-amplifier was attached to a polarising microscope which was connected to the computer via a digital oscilloscope. An AC triangular wave of varying amplitude and different frequencies was applied to the cells for this purpose. For a 2-μm cell, alignment was achieved by slowly cooling the sample to the smectic mesophase and simultaneously applying a sine wave electric field (10 V/μm). The sample cell was placed between crossed polarisers, with the smectic layer normal, parallel to one of the polarisers in the absence of any external electric field.

For the dielectric measurements, ITO-coated, planar-aligned EHC cells of 10-μm thickness were used. The temperature of the cells was controlled by a Mettler FP52 Hot Stage attached to a FP5 temperature control unit. Dielectric data were recorded in the frequency range from 10 Hz to 13 MHz using a HP4192 Impedance Analyzer in both heating and cooling cycles. Since the dielectric loss spectra of the sample have a comparatively high dc loss at the low-frequency end and are also asymmetric, the frequency dependence of the complex dielectric permittivity ε* can be better described by the superposition of the Havriliak–Negami [28] fit function and a conductivity contribution. Characteristic dielectric parameters such as dielectric strength and relaxation frequency were extracted after incorporating the dielectric data into the following extended Havriliak–Negami function equation:

$$\varepsilon'' = \frac{\sigma_0}{\varepsilon_0}.\frac{1}{\omega^s} + \sum_{k=1}^{N} \mathrm{Im}\left\{\frac{\Delta\varepsilon_k}{\left[1+(i\omega\tau_k)^{\alpha_k}\right]^{\beta_k}}\right\} \qquad (1)$$

where $\Delta\varepsilon_k$ is the dielectric strength, $\tau_k$ is the relaxation time of each individual process $k$ involved in dielectric relaxation, $\varepsilon_0$ (8.854 pF $m^{-1}$) is the vacuum permittivity, and $\sigma_0$ is the conduction parameter. The exponents $\alpha$ and $\beta$ are empirical fit parameters, which describe a symmetric and a non-symmetric broadening, respectively, of the relaxation peaks. The first term on the right-hand side of equation (1) describes the motion of free charge carriers in the sample. In the case of Ohmic behaviour ($s = 1$) $\sigma_0$ is the Ohmic conductivity of the smectic material.

## 3. Results and discussion

### *3.1 Dielectric studies*

The temperature dependence of real part of dielectric permittivity $\varepsilon'$ (T) (Figure 2(a) and (b)) revealed the existence of another phase in the temperature range between 78.6 and 92.0°C in the OAFLC in our study during heating. During cooling, no such phase was found in the temperature range mentioned above.

The dielectric spectrum shows complex behaviour during heating. In the temperature range between 78.6 and 92°C, three peaks were observed corresponding to the three relaxation processes in the dielectric spectra (Figure 3). Above 92°C and up to 108°C, the temperature of transition ($T_C$) from the SmC* to the SmA* phase, a single peak was observed in the dielectric spectrum (Figure 3).

However, during cooling throughout the temperature range above, even below 78°C, a single peak was observed due to the Goldstone mode (GM) process. The GM was observed during cooling from 107°C down to 70°C. Its strength (≅100) and relaxation frequency are almost independent of temperature; this is characteristic behaviour of the GM process. The SmC* phase has been extended by a few degrees inside the $SmC_A$* phase. By comparing the GM dielectric strength during cooling and heating we can assign

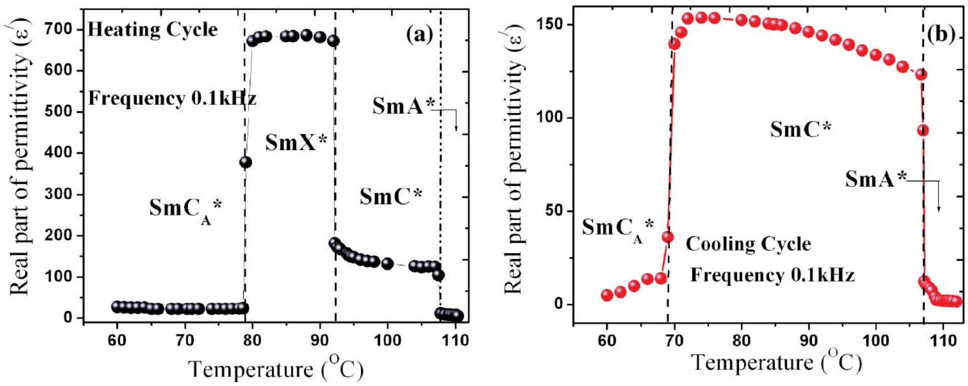


Figure 2. Variation of real part of dielectric permittivity (ε′) with temperature in a 10-μm cell during (a) heating and (b) cooling cycles.

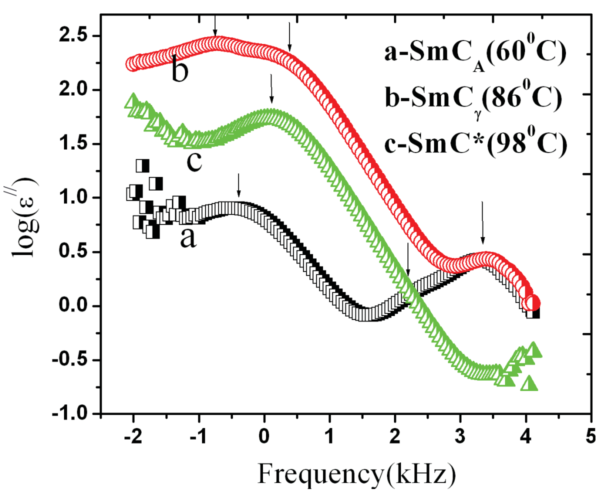


Figure 3. Variation of imaginary part of dielectric permittivity (ε″) with frequency in a 10-μm cell during heating.

the SmC* phase during heating in the temperature range between 107.5 and 92°C, and below 92°C there was again a sharp increase in dielectric strength (Figure 4(a)) which was much higher than the GM strength. Recently, Cepic *et al.* [29] developed a phenomenological theory describing the dynamic behaviour and the dielectric spectra of different SmC$_A$* subphases. This model predicts that below the phase transition temperature SmC* → SmC$_\gamma$* the dielectric strength of the phason mode increases and relaxation time decreases by one to two orders of magnitude. The increase in GM strength in the SmC$_\gamma$* phase in comparison to that in the SmC* phase was previously reported by Uehara *et al.* [30] and Lagerwall *et al.* [31]. Therefore, from the above considerations, we can identify the range from 92.0 to 78.6°C as a new phase and that can be identified as the SmC$_\gamma$* phase which is extremely sensitive with respect to the cell conditions, aligning material, etc., and which did not appear in earlier studies [9] in a 5-μm cell due to the suppression of this phase in thin cells. Three dielectric modes are observed in this phase, two in the low frequency region and another one in the high frequency region (Figure 4(b)). The lowest frequency mode, which was observed around 350 Hz, is much lower than the GM relaxation frequency and can be assigned as the ferroelectric GM, while the other frequency, observed at around 2 kHz, coincides with the GM relaxation frequency

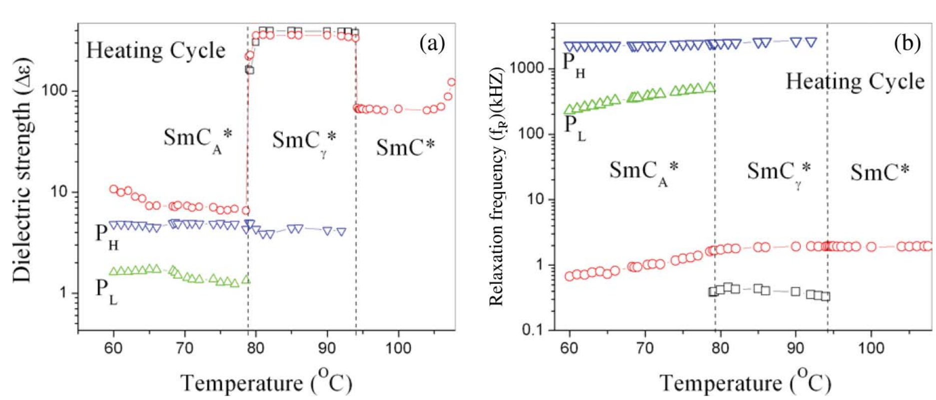


Figure 4. Temperature dependence of (a) dielectric strength (Δε) and (b) relaxation frequency ($f_R$) in a 10-μm cell during the heating cycle.

(Figure 4(b)). The existence of this mode is assumed to be the ferroelectric GM in the SmC$_\gamma$* phase. The relaxation frequency of the mode that has been observed in the high-frequency region coincides with one of the high-frequency antiferroelectric modes. Previously, Hiraoka *et al.* [32] also observed a mode in the megahertz region in the SmC$_\gamma$* phase. The existence of these processes can possibly be explained by the importance of the antiferroelectric interactions in the SmC$_\gamma$*phase. The mechanism of the three relaxation processes in the SmC$_\gamma$* phase can be well understood for the reasons we describe in the following.

Considering the twisting power and circular dichroism measurements, Lee *et al.* [33] suggested that the ferroelectric phase was found to be composed of ferroelectric and antiferroelectric structures in the ratio of 3:7. Therefore, apart from the characteristic ferrielectric GM, the SmC$\gamma$* phase also possesses the ferroelectric GM and antiferroelectric mode.

In the antiferroelectric SmC$_A$* phase, three absorption peaks were present as can be seen in the dielectric spectrum of the material (Figure 3). We can assign two peaks as $P_L$ and $P_H$ modes which are separated from each other by almost one frequency decade (Figure 4(b)). The $P_L$ mode originates due to the collective reorientation of the molecules around their short axes and the $P_H$ mode arises due to antiphase motion of the adjacent antitilt pairs [1]. In addition to the $P_L$ and $P_H$ modes, there was another mode in the low-frequency region throughout the SmC$_A$* phase. The dielectric strength of this mode is higher than that of the $P_L$ and $P_H$ modes and the relaxation frequency is around 1 kHz (Figure 4(a) and (b)). Previously, many researchers observed this kind of mode in the antiferroelectric phase [4] and called it a hereditary peak. This mode is no doubt a collective mode since its relaxation frequency is almost independent of temperature and its strength was completely suppressed by applying an electric field of bias like that of the GM in the SmC* phase. This should be the Goldstone-like mode in the SmC$_A$* phase and reveals the coexistence of ferroelectric and antiferroelectric orders [19] in the low-temperature phase. In an earlier study of this material, Perkowski *et al.* [9] identified this mode as $P_L$. They denoted the highest frequency (~106 Hz) mode as the X mode and the mode around 105 Hz as the $P_H$ mode in the SmCA* phase. However, the origin of the X mode was not clearly explained. We believe that the X mode is actually the $P_H$ mode and that which is observed around 105 Hz is the $P_L$ mode, by comparing our results with that of Buivydas *et al.* [1]. It should be noted that the $T_C$ has been shifted at the higher-temperature side by 1°C in the thin (4-μm) cell due to the confinement effect, which is in agreement with the earlier observation by Dierking *et al.* [34] for the SmC* → SmI* transition. The occurrence of the SmC$_\gamma$* phase during heating is obviously due to antiferroelectric interaction within a certain temperature range in the SmC* phase. Finally, it can be observed that the phase sequence obtained from the dielectric measurements is

$$\mathrm{Cr}<57.5\,^\circ\mathrm{C}\ \mathrm{SmC_A}^*\ 78.6\,^\circ\mathrm{C}\ \mathrm{SmC_\gamma}^*\ 92\,^\circ\mathrm{C}\ \mathrm{SmC}^*\ 107.6\,^\circ\mathrm{C}\ \mathrm{SmA}^*\ 114.9\,^\circ\mathrm{C}\ \mathrm{Iso}$$

during the heating cycle and

$$\mathrm{Cr}<57.5\,^\circ\mathrm{C}\ \mathrm{SmC_A}^*\ 70\,^\circ\mathrm{C}\ \mathrm{SmC}^*\ 107.6\,^\circ\mathrm{C}\ \mathrm{SmA}\ 114.9\,^\circ\mathrm{C}\ \mathrm{Iso}$$

during the cooling cycle, which differ from that obtained from the DSC study.

### *3.2 Electro-optical studies*

The material under investigation in the present article is an OAFLC material; the tilt angle is quite high, around 44.51° at 60°C. The tilt angle slowly decreases with increasing temperature and becomes ~26.65° at 109.2 °C (SmC* → SmA* transition); see Figure 5. Since the AFLC molecule possesses a highly polar fluorinated group at the meta-position, it contributes a high dipole moment in the transverse direction. Thus, it possesses a large spontaneous polarisation, ~240 nC cm$^{-2}$ at 60°C (Figure 5), which closely corresponds to the value reported by other researchers [35]. The value of $P_S$ slowly decreases with increasing temperature. The electrical switching time (Figure 6)

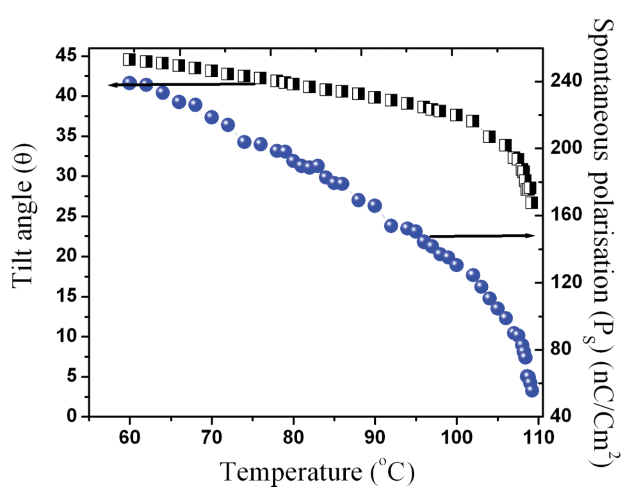


Figure 5. Temperature dependence of tilt angle ($\theta$) and spontaneous polarisation ($P_S$) in a 10-μm cell.

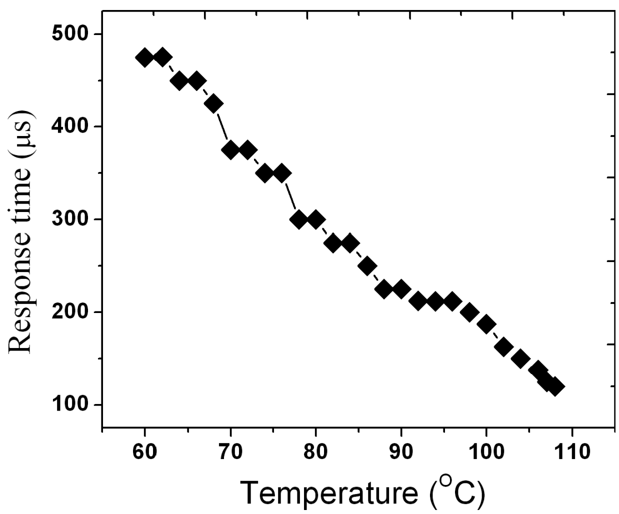


Figure 6. Temperature dependence of response time in a 10-μm cell in the antiferroelectric and ferroelectric phases.

gradually decreases with the increase of temperature and it is around 150 μs in the SmC* phase.

### 3.2.1 *Optical switching*

Optical transmission was recorded at different temperatures, i.e. at different smectic phases (Figure 7), by varying voltages and frequencies in the 2-μm (EHC) cell. We observed an ideal threshold-less, hysteresis-free, V-shaped switching in the ferroelectric SmC* phase. In a 2-μm cell a homogeneous alignment was achieved by very slow cooling and by simultaneously applying a low-frequency electric field (5 V μm$^{-1}$ and 20 Hz). An application of a low-frequency field during cooling may enhance polar anchoring which is a necessary requirement to achieve V-shaped switching. V-shaped switching in the SmC* phase is caused by the field-induced switching of a non-equilibrium twisted SmC* phase stabilised by the polar

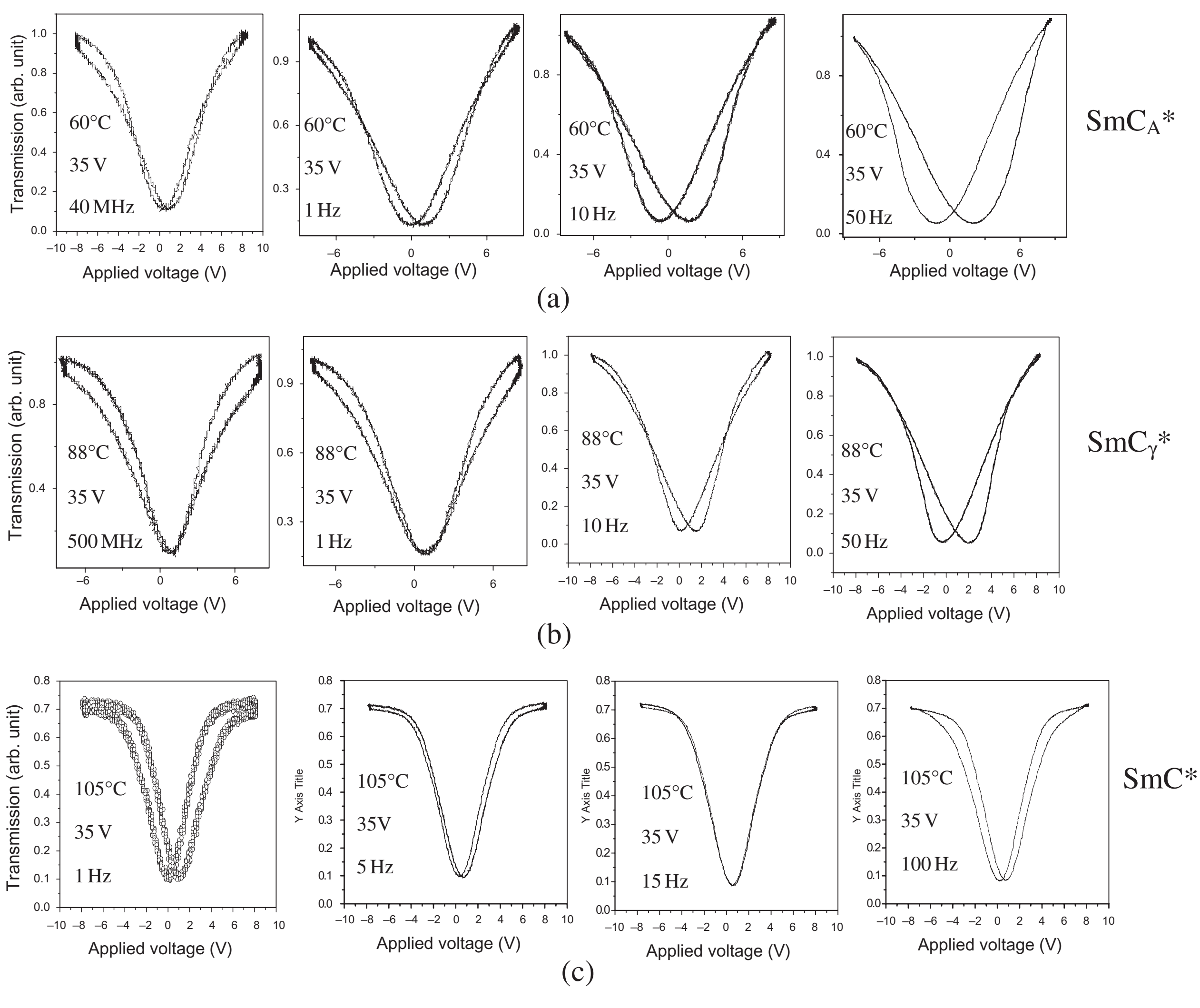


Figure 7. Optical transmission versus voltage at temperatures (a) 60°C, (b) 88°C and (c) 105°C in a 2-μm cell.

surface interaction and by the electrostatic bulk polarisation charge (splayed ferroelectric state) [19]. As shown by Figure 7(c), V-shaped switching is very sensitive to frequency and ideal V-shaped switching can be observed at a particular frequency. Optical transmittance appeared W-shaped as the frequency of the applied field is below and above a characteristic frequency, the so-called inversion frequency. This effect can be explained in terms of the accumulation of ions in the surface-stabilised AFLC cell. The alignment of $P_S$ along the external field ($E_{ext}$) results in an opposite surface field ($E_{sur}$) due to the generation of surface charges. Since $E_{sur}$ is smaller than $E_{ext}$, movements of positive and negative ions in the bulk produce another opposing field, $E_{ion}$. When the frequency of the external field is high the charges do not have the time to follow the external field and thus generate a substantial $E_{ion}$ before the external field changes sign, resulting in a normal hysteresis loop. Again, when the frequency is low the mobility of ions increases and $E_{ion}$ has strong contribution, thus a negative field exists when the external field is zero causing a hysteresis loop in the opposite sense than the one occurring at high frequency [36].

The material possesses high $P_S$ ($\sim$240 nC cm$^{-2}$ at 60°C). A high value of $P_S$ with strong polar surface interaction creates a twisted state and exhibits V-shaped switching characteristics, which is in agreement with the electrostatic model [17].



## 4. Conclusions

The newly synthesised OAFLC material possesses a high tilt and high spontaneous polarisation. The threshold-less, hysteresis-free, V-shaped switching was observed in the SmC* phase. Dielectric studies helped us to identify a ferrielectric SmC$_\gamma$* phase during heating, but this was absent during cooling. Instead, the SmC* phase is extended a few degrees inside the SmC$_A$* phase during cooling. We have observed a Goldstone-like mode along with two other antiferroelectric modes, the $P_L$ and $P_H$ modes, in the SmC$_A$* phase, GM in the SmC* phase, and three dielectric modes in the ferroelectric SmC$\gamma$* phase. The occurrence of the SmC$\gamma$* phase during heating is obviously due to antiferroelectric ordering into a certain temperature range in the SmC* phase.

## References


[1] Buivydas, M.; Gouda, F.; Lagerwall, S.T.; Stebler, B. *Liq. Cryst.* **1995**, *18*, 879–886.

[2] Sako, T.; Kimura, Y.; Hayakawa, R.; Okabe, N.; Suzuki, Y. *Jpn. J. Appl. Phys.* **1996**, *35*, L114–L116.

[3] Takanishi, Y.; Hiraoka, K.; Agrawal, V.K.; Takezoe, H.; Fukuda, A.; Matsushita, M. *Jpn. J. Appl. Phys.* **1991**, *30*, 2023–2027.

[4] Buivydas, M.; Gouda, F.; Andersson, G.; Lagerwall, S.T.; Stebler, B.; Gestblom, B. *Liq. Cryst.* **1997**, *23*, 723–739.

[5] Hou, J.; Schacht, J.; Giesselmann, F.; Zugenmaier, P. *Liq. Cryst.* **1997**, *22*, 409–417.

[6] Lagerwall, J.P.F.; Rudquist, P.; Lagerwall, S.T. *Liq. Cryst.* **2003**, *30*, 399–414.

[7] Chandani, A.D.L.; Ouchi, Y.; Takezoe, H.; Fukuda, A. *Jpn. J. Appl. Phys. Lett.* **1989**, *28*, L1261–L1264.

[8] Fukui, M.; Orihara, H.; Yamada, Y.; Yamamoto, N.; Ishibashi, Y. *Jpn. J. Appl. Phys. Lett.* **1989**, *28*, L849–L850.

[9] Perskowski, P.; Ogrodnik, K.; Lada, D.; Piecek, W.; Rutkowska, J.; Raszewski, Z.; Urowska, M.; Dabrowski, R.; Sun, X. *Opto-Electron. Rev.* **2008**, *16*, 277–280.

[10] Fukuda, A. In *Pretransitional Effect in AF-F Switching: To Suppress It or to Enhance It, That is the Question About AFLCDs,* Proceedings of 15th International Display Research Conference, Asia Display '95, Hamamatsu, Japan, October 16–18, 1995; Society for Information Display: San Jose, CA, 1995.

[11] Inui, S.; Iimura, N.; Suzuki, T.; Iwane, H.; Miyachi, K.; Takanishi, Y.; Fukuda, A. *J. Mater. Chem.* **1996**, *6*, 671–673.

[12] Clark, N.A.; Lagerwall, S.T. *Appl. Phys. Lett.* **1980**, *36*, 899–901.

[13] Fukuda, A.; Takanishi, Y.; Isozaki, T.; Ishikawa, K.; Takezoe, H. *J. Mater. Chem.* **1994**, *4*, 997–1016.

[14] Lee, J.; Chandani, A.D.L.; Itoh, K.; Ouchi, Y.; Takezoe, H.; Fukuda, A. *Jpn. J. Appl. Phys.* **1990**, *29*, 1112–1127.

[15] Chandani, A.D.L.; Hagiwara, T.; Suzuki, Y.; Ouchi, Y.; Takezoe, H.; Fukuda, A. *Jpn. J. Appl. Phys.* **1988**, *27*, L729–L732.

[16] Seomun, S.S.; Park, B.; Chandani, A.D.L.; Hermann, D.S.; Takanishi, Y.; Ishikawa, K.; Takezoe, H.; Fukuda, A. *Jpn. J. Appl. Phys.* **1998**, *37*, L691–L693.

[17] Clark, N.A.; Coleman D.; Maclennan, J.E. *Liq. Cryst.* **2000**, *27*, 985–990.

[18] Rudquist, P.; Maclennan, J.E.; Shao, R.; Link, D.R.; Walba, D.M.; Clark, N.A. Presented at the 17th International Liquid Crystal Conference 1998, P2-063, Strasbourg, France, July 19–24, 1998.

[19] Rudquist, P.; Lagerwall, J.P.F.; Buivydas, M.; Gouda, F.; Lagerwall, S.T.; Clark, N.A.; Maclennan, J.E.; Shao, R.; Coleman, D.A.; Bardon, S.; Bellini, T.; Link, D.R.; Natale, G.; Glaser, M.A.; Walba, D.M.; Wand, M.D.; Chen, X.-H. *J. Mater. Chem.* **1999**, *9*, 1257–1261.

[20] Rudquist, P.; Shao, R.F.; Coleman, D.; Bardon, S.; Link, D.R.; Bellini, T.; Maclennan, J.E.; Chen, X.H.; Walba, D.M.; Lagerwall, J.P.F.; Buivydas, M.; Gouda, F.; Lagerwall, S.T.; Clark, N.A. Presented at the 1999 SID International Symposium, San Jose, CA, May 18–20, 1999, 409–413.

[21] Park, B.; Seomum, S-S.; Nakata, M.; Takahashi, M.; Takanishi, Y.; Ishikawa, K.; Takezoe, H. *Jpn. J. Appl. Phys.* **1999**, *38,* 1474–1481.

[22] Park, B.; Nakata, M.; Seomun, S-S.; Takanishi, Y.; Ishikawa, K.; Takezoe, H. *Phys. Rev. E* **1999,** *59(4),* R3815–3818.

[23] Chandani, A.D.L.; Cui, Y.; Seomun, S.S.; Takanishi, Y.; Ishikawa, K.; Takezoe, H. *Liq. Cryst.* **1999**, *26*, 167–179.
[24] Hammarquist, A.; D'Havé, K.; Matuszczyk, M.; Clark, N.A.; Maclennan, J.E.; Rudquist, P. *Phys. Rev. E* **2008**, *77*, 031707(1–8).
[25] Blinov, L.M.; Palto, S.P.; Pozhidaev, E.P.; Bobylev, Y.P.; Shoshin, V.M.; Andreev, A.L.; Podgornov, F.V.; Haase, W. *Phys. Rev. E* **2005**, *71*, 051715.
[26] Manjuladevi, V.; Panarin, Y.P.; Vij, J.K. *Appl. Phys. Lett.* **2007**, *91*, 052911(1–3).
[27] Morawiak, P.; Piecek, W.; Żurowska, M.; Perkowski, P.; Raszewski, Z.; Dabrowski, R.; Czuprynski, K.; Sun, X.W. *Opto-Electron. Rev.* **2009**, *17*, 40–44.
[28] Havriliak, S; Negami, S. *J. Polym. Sci.: Part C* **1966**, *14*, 99–117.
[29] Cepic, M.; Heppke, G.; Hollidt, J.M.; Lotzsch, D.; Zeks, B. *Ferroelectrics* **1993**, *147*, 159–170.
[30] Uehara, H.; Hanakai, Y.; Hatano, J.; Saito, S.; Murashiro, K. *Jpn. J. Appl. Phys.* **1995**, *34*, 5424–5428.
[31] Lagerwall, J.P.F.; Dabrowski, R.; Scalia, G. *J. Non-Cryst. Solids* **2007**, *353*, 4411–4417.
[32] Hiraoka, K.; Taguchi, A.; Ouchi, Y.; Takezoe, H.; Fukuda, A.J. *Jpn. J. Appl. Phys.* **1990**, *29*, L103–L106.
[33] Lee, J.; Ouchi, Y.; Takezoe, H.; Fukuda, A.; Watanabe, J. *J. Phys.: Condens. Matter* **1990**, *2*, 271–274.
[34] Dierking, I.; Ghosh, A.K.; Haase, W. *J. Phys.: Condens. Matter* **2002**, *14*, 13441–13448.
[35] Lagerwall, J.P.F.; Saipa, A.; Giesselmann, F.; Dabrowski, R. *Liq. Cryst.* **2004**, *31*, 1175–1184.
[36] Petrenko, A.; Goodby, J.W. *J. Mater. Chem.* **2007**, *17*, 766–782.